Hindawi
Journal of Nanomaterials
Volume 2022, Article ID 1760198, 15 pages
https://doi.org/10.1155/2022/1760198

Research Article

Carbon Nanotube-Based Reinforced Polymers for Medical Applications: Improving Impact Strength of Polymer-Polymer Composites

Marwah AL-Maatoq,[1] **Patricio Fuentealba**,[2] **Melanie Fachet**,[1] **Rainer Glüge**,[3] **Salah H. R. Ali**,[4] **and Christoph Hoeschen**[1]

[1]*Faculty of Electrical Engineering and Information Technology, Institute for Medical Technology, Chair of Medical Systems Technology, Otto von Guericke University, Magdeburg 39106, Germany*
[2]*Faculty of Engineering Sciences, Institute of Electrical and Electronics Engineering, Austral University of Chile, Valdivia 5090000, Chile*
[3]*DB Netz AG, Maybachstr. 26, Magdeburg D-39104, Germany*
[4]*Engineering and Surface Metrology, Dept., Precision Engineering Division, National Institute for Standard (NIS), Al-Haram, Tersa St, Giza 12211-136, Egypt*

Correspondence should be addressed to Marwah AL-Maatoq; marwah.al@ovgu.de

Received 16 June 2021; Revised 18 February 2022; Accepted 7 March 2022; Published 1 April 2022

Academic Editor: Bhanu P. Singh

There is a continuous need for innovative biomaterials with advanced properties to meet the biomechanical requirements of orthopedic implants and interventional devices. Recent research findings show that using material composites leads to significantly improved properties, which are beneficial for medical applications. Therefore, this work aims at studying polymer-polymer composites of high-density polyethylene (HDPE) and ultrahigh molecular weight polyethylene (UHMWPE), which were mixed with and without reinforcement of multiwall carbon nanotubes (MWCNTs) in two steps. An extensive characterization workflow including mechanical tensile tests, tribological performance, and surface characteristics was used to analyze the reinforced polymer-polymer composite samples. The results of the mechanical tests showed that the developed MWCNT-reinforced samples achieved better performance, due to a higher yield point that is the highest in the sample with 48.5% HDPE-50% UHMWPE-0.5% MWCNTs, a higher value in the hardness test peaking in the sample with 49.5% HDPE-50% UHMWPE-0.5% MWCNTs, and a lower friction coefficient in HDPE-UHMWPE-MWCNTs samples. Overall, the reinforcement of polymer-polymer composites with MWCNTs led to a significant improvement of the material characteristics required for the designated use in orthopedic implants and interventional biopsy needles, which will lead to improved clinical results.

1. Introduction

In recent decades, synthetic polymeric composites have gained increased interest in biomaterials, due to their capability to enhance the mechanical properties of biomaterials to solve several medical needs [1–8]. Synthetic polymeric composites have important properties required for medical applications, which are biofunctionality, biocompatibility, and manufacturability [2, 9]. In addition, the structure of individual polymeric composites consists of two separate components attempting to achieve several beneficial characteristics, such as reduced weight, improved mechanical and physical properties, and reasonable costs [10–13]. Moreover, they have the capability to fulfill certain dimensional and shape requirements for application areas with complex geometries, such as the orthopedic implants [14–16] and

the design of biopsy needles [17, 18]. Currently, around twenty types of synthetic polymeric biomaterials are available and used for a large variety of medical applications. Among those, the most common type is polyethylene (PE), which is commercially available in five major types: (1) high-density polyethylene (HDPE), (2) low-density polyethylene (LDPE), (3) linear low-density polyethylene (LLDPE), (4) very low-density polyethylene (VLDPE), and (5) ultra-high molecular weight polyethylene (UHMWPE) [19]. Particularly, UHMWPE shows a low friction coefficient and high wear resistance and impact strength. Therefore, it is commonly used as bearing materials with ceramic or metallic counter surfaces in joint arthroplasty [20]. While HDPE shows a better creep resistance but a lower wear resistance, it can be blended with UHMWPE to enhance the creep resistance [21]–[24].

Nonetheless, there is a continuous demand to improve the mechanical and tribological properties of synthetic polymeric biomaterials in general and UHMWPE and HDPE in particular to provide durable orthopedic implants for patients [25–28]. Therefore, two approaches are commonly used to improve the UHMWPE and HDPE performance, which is crosslinking and reinforcement [21, 29]. The reinforcement of UHMWPE is often realized by addition of particles or nanofillers, such as titanium dioxide (TiO_2), aluminum oxide (Al_2O_3), graphene, silica nanoparticle, and carbon nanotubes (CNTs) [27, 30–35].

It was found that the polymers reinforced with nanofillers have a higher strength to mass ratio and they have been used to reinforce the structure, specifically in the areas of the blade, where there is a high mechanical load [36]. In addition, adding nanofillers has a synergetic effect on polymer-polymer composites [37].

Therefore, the concept of particle reinforcement is the most promising approach for improving UHMWPE and HDPE, because it leads to beneficial mechanical and tribological properties, such as low friction and high wear resistance and supporting thermoset resins [8, 38, 39]. CNTs are used as reinforcement material in polymeric-based composites due to their promising mechanical properties, such as high tensile modulus, high strength, and increase of the load bearing capacity up to 12 N [40, 41]. Moreover, CNTs have a very high ratio of surface area over volume due to their nanoscale diameter [42, 43].

In general, CNTs come in different forms, for instance single-wall carbon nanotubes (SWCNTs), double-wall carbon nanotubes (DWCNTs), and multiwall carbon nanotubes (MWCNTs) [43, 44]. Especially, chemical and physical properties of MWCNTs have shown better behavior when developing orthopedic implants [45, 46]. However, very limited work has been reported on polymeric reinforced with MWCNTs for improvement of mechanical and tribological properties. The main contribution of this work is to investigate the role of adding MWCNTs as a reinforcement material for two synthetic polymers, namely, HDPE and UHMWPE, by thorough mechanical and tribological tests to optimize their performance. This goal is achieved by the fabrication of 21 samples in two-stage polymeric composites containing a specific mixture of HDPE and UHMWPE with and without the addition of MWCNTs. The main objective of this work is to compare the material characteristics and sample performance of polymer-polymer composites with and without addition of MWCNTs for medical applications. The concept of reinforced UHMWEP-HDPE mixtures with CNTs has been proposed in several publications [21, 34, 35, 47–49]. However, these studies only provide a limited number in proposed polymeric composite samples for testing. In addition, there is lack of applying the complete mechanical tensile test to the samples. Therefore, the novelty is to provide a detailed analysis for 21 samples using a comprehensive workflow to optimize the mechanical properties via the fabrication process of mixing polymeric matrix (HDPE-UHMWPE) reinforced with mixing ratio of MWCNTs in powder forms. The proposed samples consist of an extensive sample composition range combined with a detailed characterization of mechanical, tribological, and surface properties that is currently not available in the literature to this extent.

2. Materials and Methods

Three types of raw materials have been used in this work for sample preparation: HDPE, UHMWPE, and MWCNTs. HDPE (type B4660) was purchased from SABIC Company (Saudi Arabia) and UHMWPE (type UHMWPE500) and MWCNTs (purity >95%) from LUOYANG GUORUN PIPES CO., LTD (China). In this work, two types of samples were fabricated, the first sample group was made from pure HDPE-UHMWPE mixtures. The second group was fabricated by adding MWCNTs in various concentrations to selected sample compositions from the HDPE-UHMWPE group with the most promising mechanical properties according to the evaluation strategy described in the following sections.

2.1. Manufacturing Process. Figure 1 presents a schematic illustration of the proposed workflow for sample preparation and evaluation. It consists of a mixing and weighting process for the sample composition with different ratios of HDPE-UHMWPE as shown in Table 1 and for HDPE-UHMWPE-MWCTNs in Table 2. Subsequently, a melting extrusion step using an extrusion device (Lab Extruder, Neoplast Company, India) was performed for mixing the proposed samples applying a temperature of 220°C and an extrusion speed of 220 rpm. The melting extrusion was set to 220°C, because it is essential to adequately heat the polymer mold above the melting temperature, maintain that temperature and thoroughly stir the mold. This is necessary to dissolve any solidification nuclei that persist in the mold [50]. Afterward, a molding step was applied to both sample groups, using a plastic injection molding machine (MI MORGAN-PRESS, USA) with a temperature of 250°C and a sample dimension of $10\,cm \times 1\,cm \times 0.4\,cm$ (length, width, and height).

2.2. Evaluation Strategy. The evaluation strategy of this study was based on mechanical tests, surface characteristic measurements, and tribological tests for the determination of the friction coefficients. First, the mechanical sample

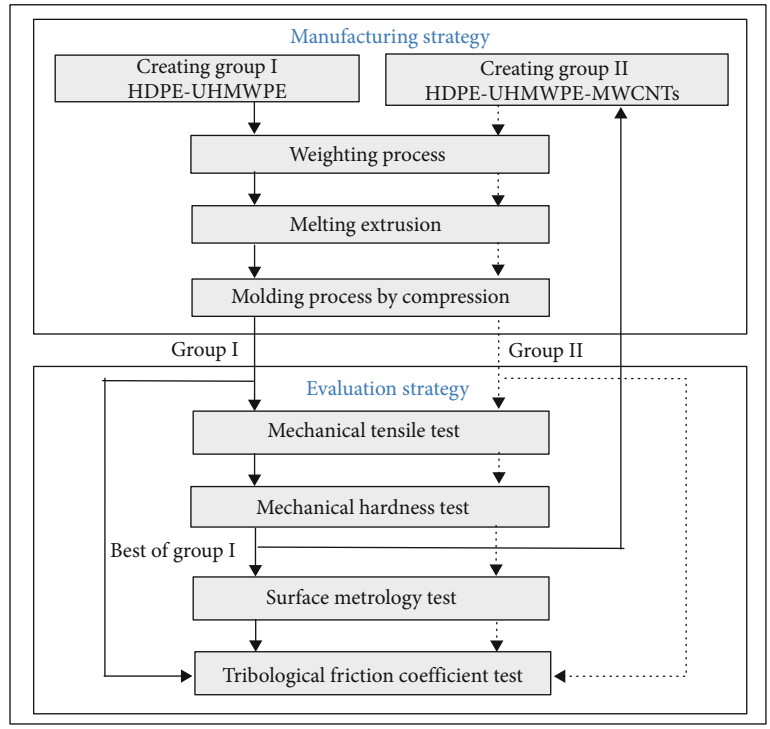

Figure 1: Schematic drawing of the mechanical and tribological workflow applied in this work for preparation and evaluation of the proposed samples.

Table 1: Sample composition in percentage (%) for the proposed composites based on high-density polyethylene (HDPE) and ultrahigh molecular weight polyethylene (UHMWPE) polymers.

Group I samples	HDPE (%)	UHMWPE (%)
1	100	0
2	90	10
3	80	20
4	70	30
5	60	40
6	50	50
7	40	60
8	30	70
9	20	80
10	10	90
11	0	100

evaluation consists of tensile and hardness measurements. The mechanical tensile test represented in a stress-elongation curve consists of three main features known as the yield point, the ultimate tensile strength, and the fracture tensile strength. The yield point represents the maximum limit where the sample still can be elastic [51, 52]. The elastic region is the area prior to the yield point where the sample can return back to its original shape after removing the load, which is represented by Young's modulus [53, 54]. While the ultimate stress represents the plastic region for the sample elongation [55, 56]. Fracture stress is the state of material where the sample elongates and then separates into two pieces under the action of tension applied by the tensometer [56]. The mechanical tensile test was performed with a tensometer (Xforce HP, S/N: 755571, Zwick/Roell, Germany) under room conditions (temperature $23 \pm 2^{\circ}C$ and relative humidity $50 \pm 5\%$) using a force load cell according to a standard operating procedure (ASTM D638-03 (2014)). Briefly, the tested sample was placed between two grips of movable and stationary fixtures that pull the sample until it breaks by measuring the applied load versus the sample elongation.

The second step proposed in the evaluation strategy was the mechanical hardness test, which determines the material properties and gives a valuable insight into the strength of the composites. The hardness test was performed using a hardness tester (Shore D scale, Zwick/Roell, Germany). The hardness test was conducted under room temperature ($23 \pm 2^{\circ}C$) and relative humidity ($45 \pm 5\%$), respectively. The test was performed according to the standard operating procedure (ASTM D2240-05 (2010)) with the Shore D scale to quantify the results of the proposed samples [57]. The hardness tester records the measurements by using a durometer and it has an indenter that is pressed into the samples. The readings are recorded according to the resistance of the polymer body to the indenter. A higher value of hardness is related to a higher resistance to the indenter, whereas a higher shore recorded in the gauge is related to more stiffness of the sample.

Accordingly, mechanical tensile and hardness tests were employed to evaluate the best performing sample for the HDPE-UHMWPE mixture from Table 1. Afterwards, HDPE-UHMWPE-MWCNT samples were fabricated, based

Table 2: Proportion of HDPE-UHMWPE-MWCNT composites for the proposed samples in percentage (%).

Group II samples	HDPE (%)	UHMWPE (%)	MWCNTs (%)
12	49.5		0.5
13	49.0		1.0
14	48.5		1.5
15	48.0		2.0
16	47.5	50.0	2.5
17	47.0		3.0
18	46.5		3.5
19	46.0		4.0
20	45.5		4.5
21	45.0		5.0

on the selected samples from the HDPE-UHMWPE group, and evaluated using the workflow described above.

A surface metrology test was performed to determine the surface characteristics of the fabricated samples [58, 59]. A sample was selected from each group according to their mechanical performance and was characterized in order to observe the homogeneity of CNT distribution in the fabricated samples. The test was performed by scanning electron microscopy (SEM, JSM 6300F, USA). All SEM samples must be electrically conductive; therefore, the sample was first fixed as a thin film by a carbon tape in substrate copper with dimensions of $(L \times W \times H)$ $(10\,mm \times 3\,mm \times 2\,mm)$. The second step was to cover the sample by a fine coating device using a gold-ion sputtering coating that includes an alloy of gold ions used for the coating. The third step was to pass the sample to a critical point dryer to remove humidity from the sample, while the last step was to attach the substrate copper with the sample to the SEM holder to do the scanning and to record the images. Furthermore, the last stage in the evaluation strategy was a tribological test for determining the friction coefficient of the sample from each group at static position. This was accomplished by an inclined plane set up to distinguish the performance of the friction when the samples are with and without MWCNTs.

3. Results and Discussion

3.1. Mechanical Characterization of Polymer Composites with and without MWCNT Reinforcement. The results of the mechanical performance evaluation based on tensile test and hardness test are described and discussed in detail below.

3.2. Mechanical Tensile Test for HDPE-UHMWPE Samples. The results for the mechanical tensile test applied to the HDPE-UHMWPE samples are shown in Figure 2, and the results, including the uncertainty assessment of the six tensile properties based on the mean ($\bar{X}$ of the data and its standard deviation (SD), are presented in Table S1 (Supplementary section). Concerning Young's modulus measurements presented in Figure 2(a), 20% HDPE-80% UHMWPE achieved the highest performance with a value of 744.47 ± 353.64 MPa. Young's modulus showed an ascending trend from mixture 50% HDPE-50% UHMWPE up to 10% HDPE-90% UHMWPE. It was observed that the sample composed of pure 100% HDPE and pure 100% UHMWPE showed approximately the same values for Young's modulus. These results were in line with the literature that the pure substance of 100% HDPE presented a similar mechanical performance to the sample composed of 100% UHMWPE [24]. This observation is associated with the polymer chain alignment and orientation, which did not change [60]. Moreover, it was noticed that the performance of Young's modulus increased when the concentration of HDPE decreased less than 50%, while the concentration of UHMWPE increased more than 50%. It is well known that the modulus of polymer is particularly sensitive to changes in the degree of crystallinity than any other properties. Many researchers have pointed out the correlation between modulus and crystallinity [61]. Therefore, this indicated that the sample performance supports more stress by increasing the elasticity range with the increasing UHMWPE percentage.

The results regarding the yield point for the HDPE-UHMWPE samples are shown in Figure 2(b). It was observed that the sample with 50% HDPE-50% UHMWPE showed the highest performance with a yield point at 4.65 ± 0.11 MPa. This indicated that this sample had better elastic properties compared to the other studied sample mixtures. The yield point measurements showed an increasing trend from sample 100% HDPE-0% UHMWPE on and peaked in sample 50% HDPE-50% UHMWPE. When the concentration of UHMWPE reached more than 50%, the yield point performance considerably decreased.

The results regarding the ultimate tensile strength are presented in Figure 2(c). The ultimate tensile strength was described by two parameters, the ultimate stress in MPa and the elongation at the ultimate point in percentage. The best performance was observed in the 80% HDPE-20% UHMWPE sample with a maximum force of 21.11 ± 0.40 MPa. As illustrated in Figure 2(c), the measurements showed a stable or even slightly increasing performance of ultimate stress for the first six samples.

According to literature [60], this behavior was expected, because, in this concentration range, a higher percentage of UHMWPE in the composite HDPE-UHMWPE resulted in a higher ultimate tensile strength. It is important to note that from sample 40% HDPE-60% UHMWPE on, the performance concerning the ultimate tensile strength did not follow a clear trend. This observation could be attributed to the mechanical properties of the composite itself as a result of the material mixing. In general, it has been shown that a lower concentration of HDPE results in higher tensile strength.

However, in some cases, when the primary material was the UHMWPE, a higher concentration of HPDE produced a higher tensile strength [21]. In summary, for optimal ultimate tensile strength performance, a trade-off between the two materials is required [60]. The lowest value was measured for the sample that was composed of 100%

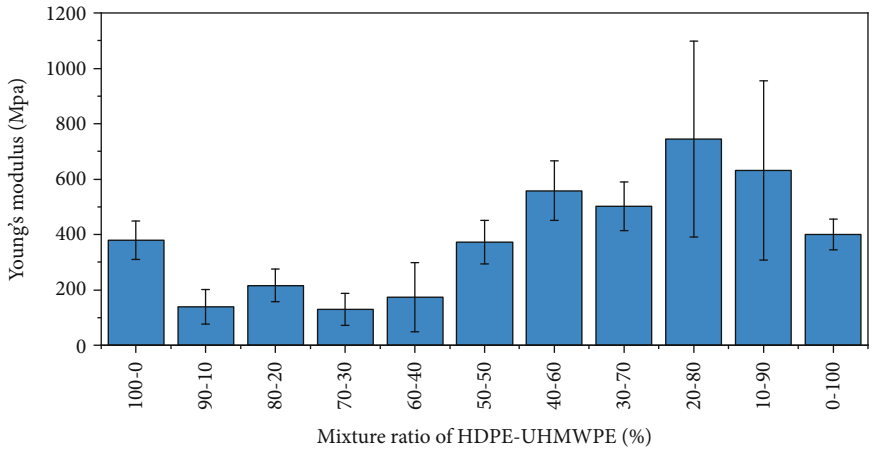

(a)

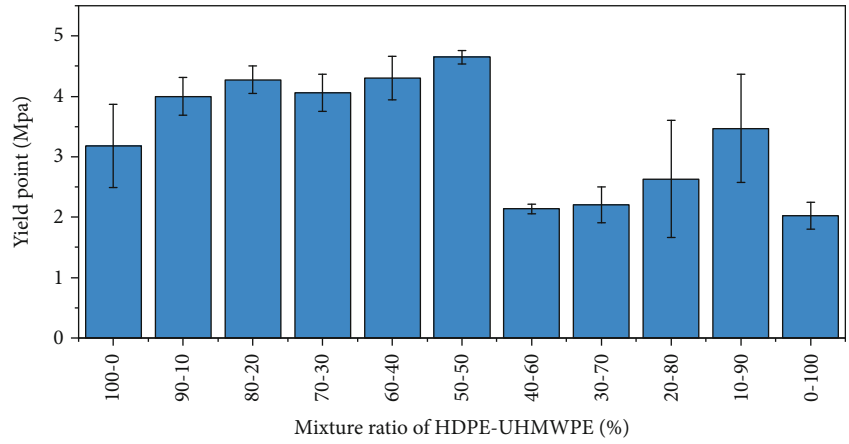

(b)

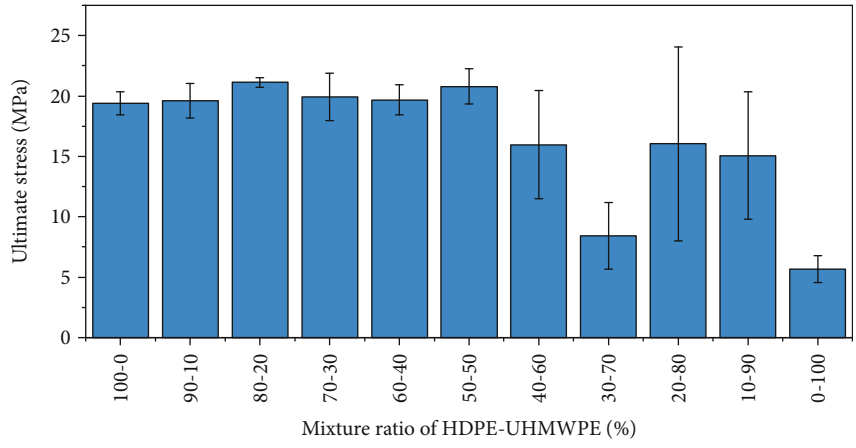

(c)

Figure 2: Continued.

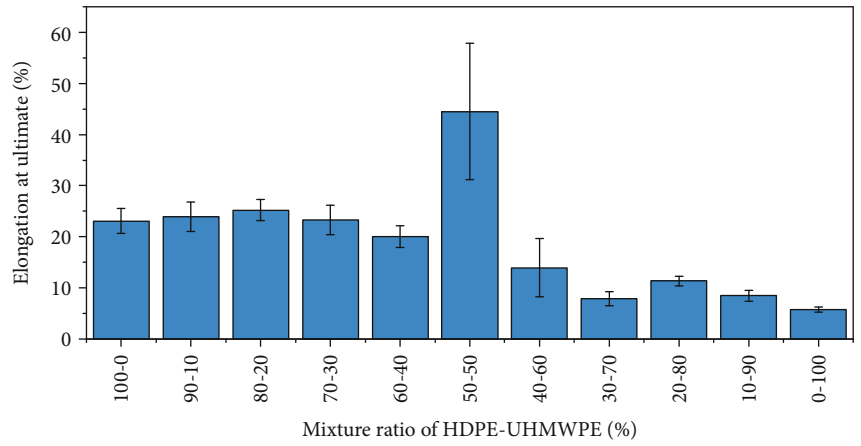

(d)

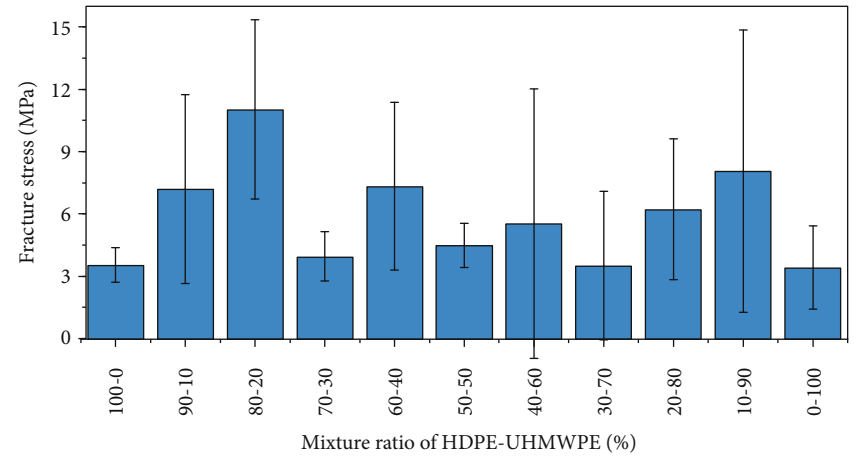

(e)

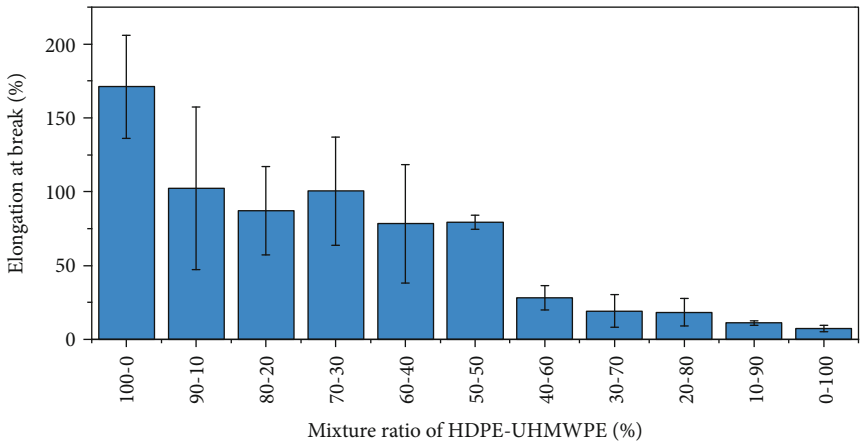

(f)

Figure 2: Results of mechanical tensile tests applied to the proposed HDPE-UHMWPE-based samples. The measurements correspond to Young's modulus (a), yield point (b), ultimate stress (c), elongation at ultimate (d), fracture stress (e), and elongation at break (f). The x-axis represents the mixing ratios used for the HDPE-UHMWPE group, while the y-axis corresponds to the physical characteristics, which are measured in unites of MPa or percentage, as appropriate. The bars (blue) and error bars (black) correspond to the mean value ($\bar{X}$ and standard deviation (SD) from five measurements, respectively.

UHMWPE, which showed the least ability to stand against ultimate force.

The second measurement involved in the ultimate tensile strength test was investigated which corresponded to the elongation of the samples, as presented in Figure 2(d). The bar chart showed a decreasing trend, except for the 50% UHMWPE-50% HDPE sample, which showed 44.49 $\pm$ 13.35% of elongation.

The results related to the fracture tensile strength are illustrated in Figures 2(e) and 2(f), fracture stress and elongation at the breaking point, respectively. Sample 80% HDPE-20% UHMWPE showed the highest value for the fracture stress which was 13.79 ± 5.52 MPa, while sample that composed of pure 100% UHMWPE showed the lowest value with 3.42 ± 1.99 MPa. For the measurements related to the elongation at the breaking point, it was observed that 100% HDPE sample showed the highest elongation with 171.04 ± 34.93%. The values of elongation at the breaking point decreased, starting from 100% HDPE sample to 100% UHMWPE sample. In summary, it was found that by increasing the UHMWPE weight fraction with decreasing the HDPE weight fraction, the elongation at the breaking point was considerably reduced.

3.3. Mechanical Hardness Test for HDPE-UHMWPE Samples. Table 3 shows the results corresponding to the hardness test applied to the HDPE-UHMWPE samples. It includes the mixing ratio for each sample in this group, whose evaluation was based on the test of five repeated measurements for each sample, as mentioned before. The results obtained from the hardness test are represented by the mean ($\bar{X}$) and standard deviation (SD) of the data. As shown in Tables 3, 50% HDPE-50% UHMWPE sample showed the highest mean value for the hardness, which was 63 ± 0.97 Shore D. This indicates that blending interactions led to significant improvements in the impact strength. While the sample composed of pure 100% UHMWPE showed the smallest value in this test, which was 54.92 ± 1.84 Shore D, and the smallest SD records in sample 60% HDPE-40% UHMWPE.

In summary, the mechanical tensile and hardness tests were performed to objectively characterize the properties of the proposed samples. In order to decide which samples showed the best performance, we based our selection on the yield point and hardness tests. These measurements represented the elasticity degree for samples in HDPE-UHMWPE before adding MWCNTs. It is important to note that the other studied measures were also necessary, which provided complementary information about the studied samples.

As a result, the measurements indicated that the best performance was achieved in the 50% HDPE-50% UHMWPE sample due to the yield point value at the mechanical tensile test and hardness test. It was caused by good interfacial interaction between the UHMWPE and HDPE phases. The crack propagation is running directly through each phase without any sign of unusual deformation at the interface, which suggests good cohesion between the UHMWPE and HDPE phases. Consequently, this sample was chosen to be the starting mixture to build the HDPE-UHMWPE-MWCNTs by adding MWCNTs as reinforcement material with the following sequence presented in Table 2.

3.4. Mechanical Tensile Test for HDPE-UHMWPE-MWCNT Samples. This section presents the results concerning the tensile test for HDPE-UHMWPE-MWCNT samples. These samples were prepared with the same strategy for the manufacturing and evaluation used for the HDPE-UHMWPE samples. It is important to note that MWCNTs were added as the third raw material to the polymeric composites (HDPE-UHMWPE). As a result, we studied ten polymeric composite samples, numbered from sample 12 to sample 21. The evaluation strategy focused on how the addition of different concentrations of MWCNTs contributed to a performance improvement compared to the composites that were purely based on HDPE-UHMWPE mixtures. The mechanical tensile measurements are shown in Figure 3, which included the same six parameters evaluated for the pure HDPE-UHMWPE samples. In parallel, Table S2 (Supplementary section) presents the results obtained from the mechanical tensile test represented by $\bar{X}$ and SD of the data.

Table 3: Results obtained from the hardness test applied to the HDPE-UHMWPE samples according to the composition (%). Presented values correspond to the mean ± standard deviation ($\bar{X}$ ± SD) of the data in (Shore D).

HDPE-UHMWPE (%)	$\bar{X}$ ± SD
100-0	60.29 ± 3.03
90-10	58.51 ± 2.68
80-20	60.39 ± 0.88
70-30	60.44 ± 0.49
60-40	61.16 ± 0.15
50-50	63.00 ± 0.97
40-60	58.52 ± 2.72
30-70	59.48 ± 1.83
20-80	60.32 ± 1.09
10-90	55.12 ± 1.84
0-100	54.92 ± 1.84

The measurement results which are shown in Figure 3(a) corresponded to Young's modulus. It was observed that in general the measurement values for the HDPE-UHMWPE-MWCNT samples are lower than those in the pure HDPE-UHMWPE samples. This indicates that the addition of MWCNTs gave the samples more stiffness.

A higher standard deviation was observed for the MWCNT-reinforced samples compared to 50% HDPE-50% UHMWPE sample without CNT reinforcement. In addition, the highest Young's modulus was observed in 47.5% HDPE-50% UHMWPE-2.5% MWCNT sample with 824.7 ± 543.03 MPa.

The yield point measurements obtained from HDPE-UHMWPE-MWCNT samples are presented in Figure 3(b). Here, it was observed that the highest point of 104 ± 28.70 MPa was measured in 48% HDPE-50% UHMWPE-2% MWCNT samples. The results showed a remarkable increase of the values compared with those of the pure HDPE-UHMWPE samples due to the ability of the proposed sample to deform elastically at high stress before it returned to its original shape.

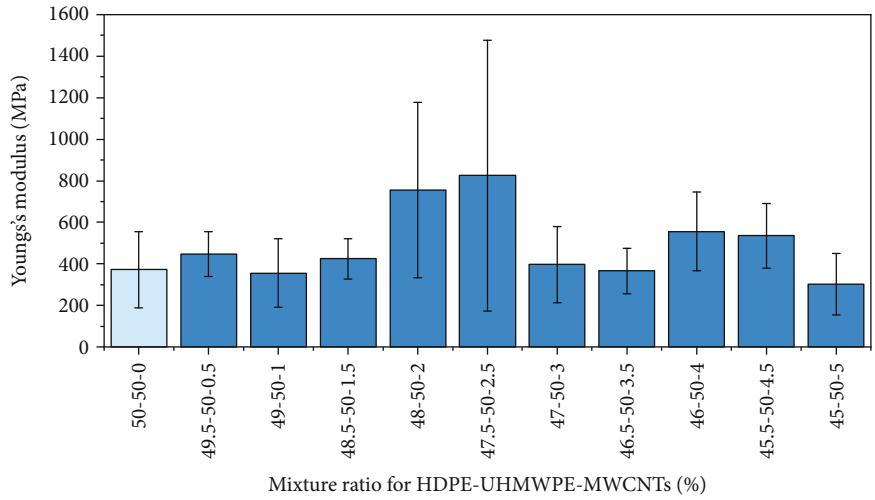

(a)

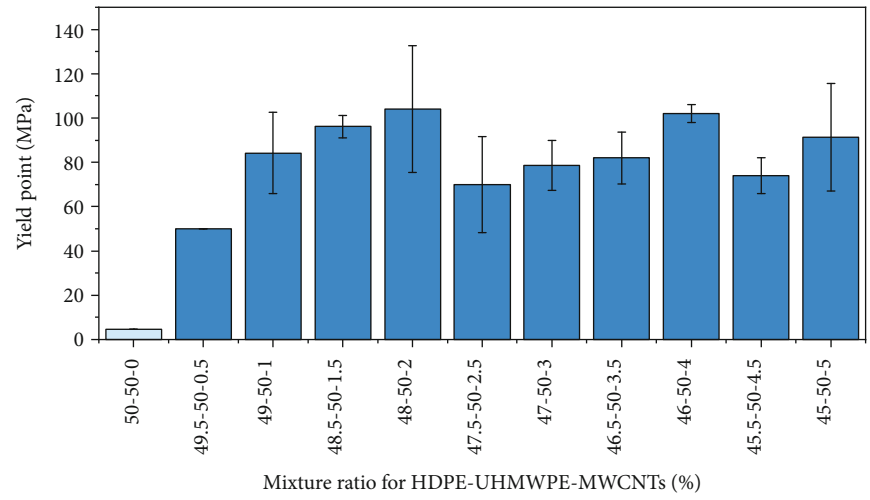

(b)

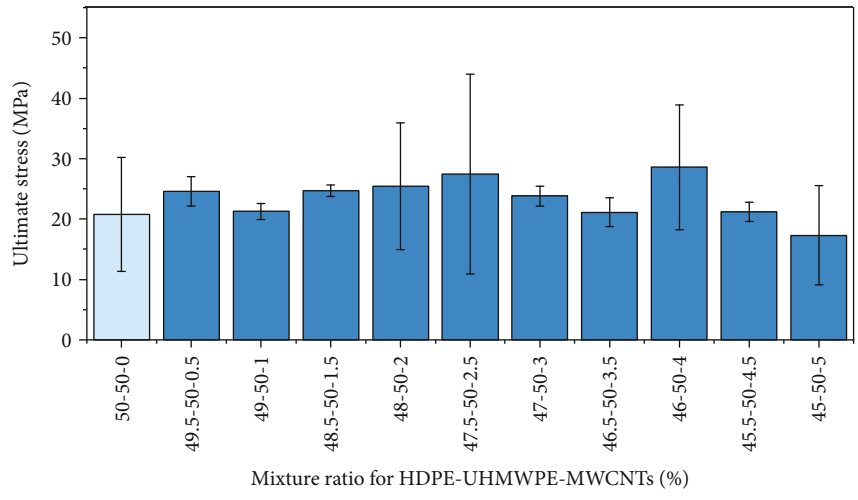

(c)

Figure 3: Continued.

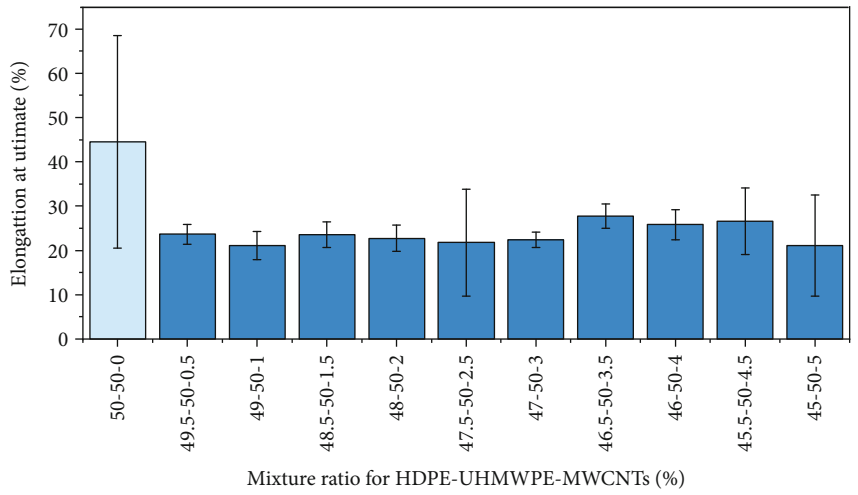

(d)

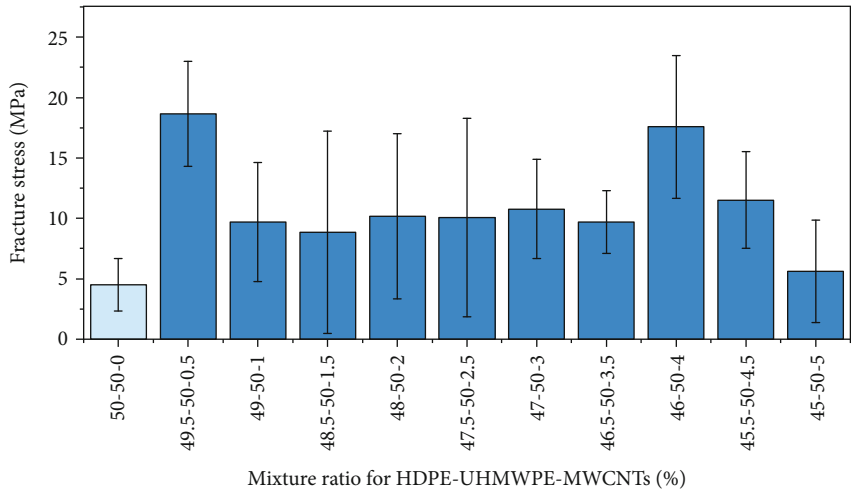

(e)

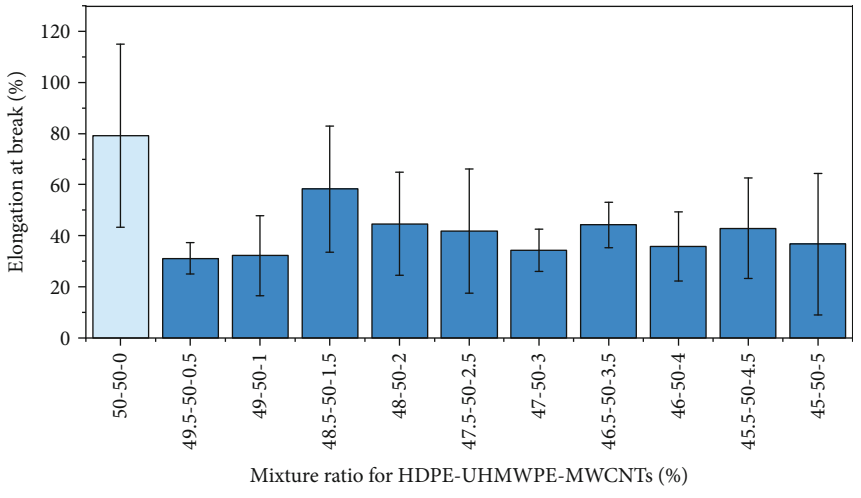

(f)

Figure 3: Results of mechanical tensile tests applied to the proposed HDPE-UHMWPE-MWCNT-based samples. The measurements correspond to Young's modulus (a), yield point (b), ultimate stress (c), elongation at ultimate (d), fracture stress (e), and elongation at break (f). The x-axis represents the mixing ratios for HDPE-UHMWPE-MWCNTs in (%), while the y-axis corresponds to the physical characteristics, which are measured in units of MPa or percentage, as appropriate. The bars (blue) and error bars (black) correspond to the mean value ($\bar{X}$ and standard deviation (SD)) from five measurements, respectively.

The results concerning the ultimate tensile strength are presented in Figure 3(c), showing that the sample composed of 46% HDPE-50% UHMWPE-4% MWCNTs had the highest performance with 28.57 ± 9.26 MPa. Moreover, it was observed that the ultimate tensile stress values were close to each other, even at different MWCNT concentrations. The lowest value corresponded to the sample composed of 45% HDPE-50% UHMWPE-5% MWCNTs with 17.30 ± 2.80 MPa. Compared to the samples of the pure HDPE-UHMWPE group, these values showed a clear increase in ultimate tensile stress when the third raw material, MWCNTs, was added. The results for the ultimate elongation are shown in Figure 3(d). The highest observed elongation was 27.74 ± 2.48 MPa for the 46.5% HDPE-50% UHMWPE-3.5% MWCNT sample.

The results related to the fracture stress measurements are presented in Figure 3(e). Here, it was observed that 49.5% HDPE-50% UHMWPE-0.5% MWCNT sample had the largest value of fracture stress, which was 18.64 ± 3.79 MPa. In contrast, the smallest value of fracture stress was found in 45% HDPE-50% UHMWPE-5% MWCNT sample with 5.63 ± 3.42 MPa. The measurements corresponding to the elongation at the breaking point are shown in Figure 3(f). These measurements showed 44.67 ± 17.98 MPa as the highest value in the sample that is composed of 48% HDPE-50% UHMWPE-2% MWCNTs and the lowest value in 49.5% HDPE-50% UHMWPE-0.5% MWCNT sample with 31.17 ± 5.47 MPa.

The stress-strain curves of the pure polymeric HDPE-UHMWPE sample and HDPE-HMWPE-MWCNT sample were compared in Figure 4. We apply the same definitions to all measurements and only compare the relative change. The secant modulus in Figure 4(a) is just stress overstrain for any curve point. Young's modulus follows from the secant modulus, it is half the initial secant modulus, which is $0.5 \times 2000\,\text{MPa} = 1000\,\text{MPa}$ for HDPE-HMWPE-MWCNT sample and $0.5 \times 1300\,\text{MPa} = 650\,\text{MPa}$ for HDPE-UHMWPE sample. Although, the yield stress follows from the definition of Young's modulus. It is a theoretical value, because the curves have no stress at which 1% of plastic strain remains when unloading along the elastic line occurs. These are the small straight lines in the stress-strain diagram at the very beginning. They start at 1% strain and then have the slope of Young's modulus. At the point where they intersect the true stress-strain curves, we define the yield limit. Meanwhile, the ultimate strain and stress are the endpoints of the curves which are 28% and 22 MPa for the HDPE-HMWPE-MWCNT sample and 25% and 19 MPa for the HDPE-UHMWPE sample. The tensile strength is the maximum stress value which is 25 MPa for the HDPE-HMWPE-MWCNT sample and 20 MPa for the HDPE-UHMWPE sample presented in Figure 4(b). This indicates that MWCNT enhances the mechanical properties and leads to provide stiffer and more ductile samples.

3.5. Mechanical Hardness Test for HDPE-UHMWPE-MWCNT Samples. The results of the hardness test applied to the HDPE-UHMWPE-MWCNT samples are shown in Table 4 including the best sample preformed from the HDPE-UHMWPE group. In this test, a sample mixture of 49.5% HDPE-50% UHMWPE-0.5% MWCNTs showed the highest hardness value with 67.02 ± 1.10 Shore D. This indicates that adding 0.5% MWCNTs to the polymeric composites translates into better creep and wear resistance. For MWCNT concentrations above 0.5%, it was noted that the hardness values plateaued between 62 and 64 Shore D. The general trend of hardness performance was showing a decrease by adding 0.5%. However, samples 14 (49% HDPE+50% UHMWPE+0.5% MWCNTs) and 16 (48.5% HDPE+50% UHMWPE+1.5% MWCNTs) have a difference in an average of 0.56%. This difference is lower than the standard deviation in Table 4.

Overall, the hardness test illustrated that samples made from HDPE-UHMWPE-MWCNTs showed considerable enhancement in the performance compared to the pure polymer-polymer composites (HDPE-UHMWPE) without reinforcement. The dispersion of MWCNTs in the matrix of polymeric composites and suitable interactions between the molecular chains and MWCNTs are key aspects of transferring the unique properties of MWCNTs to polymeric materials. Furthermore, incorporating MWCNTS reduces dissolution and improves interfacial interaction between UHMWPE-HDPE phases and acts as a bridge between the two phases at the interface region where most of the MWCNT precipitation occurs between the two phases [41, 60].

3.6. Surface Metrology Images for HDPE-UHMWPE and HDPE-UHMWPE-MWCNT Samples. A surface metrology investigation for selected samples from the polymer-polymer composites with and without reinforcement MWCNTs was performed by SEM microscopy. The microstructure of the samples was investigated by SEM imaging with different magnification factors and is presented in Figure 5. Figures 5(a), 5(b), and 5(c) refer to the pure polymeric HDPE-UHMWPE samples and show a homogeneous surface before adding MWCNTs. While the SEM for the samples with MWCNTs affects the surface behavior, most likely by acting as a cohesive agent upon cracking. The SEM image for the best sample 50% HDPE-50% UHMWPE was added in (supplementary section). Figures 5(d), 5(e), and 5(f) represent the microstructure and the distribution after addition of MWCNTs to the polymeric HDPE-UHMWPE composite.

3.7. Tribological Friction Coefficient Test for HDPE-UHMWPE and HDPE-UHMWPE-MWCNT Samples. The tribological friction coefficient test was performed on an inclined plane setup. This setup was used to relate the static friction coefficient (μ^o) to the measured value of the inclination angle (θ) when sliding starts to occur [62]. One sample from each composite group (HDPE-UHMWPE and HDPE-UHMWPE-MWCNTs) was selected for comparing the influence of CNT addition to the polymeric composite on the friction coefficient of the samples. This test was performed by sliding each sample on the inclined plane with inclination angles ranging from 0° to 30° and by using two types of surfaces. Therefore, the friction coefficient test was

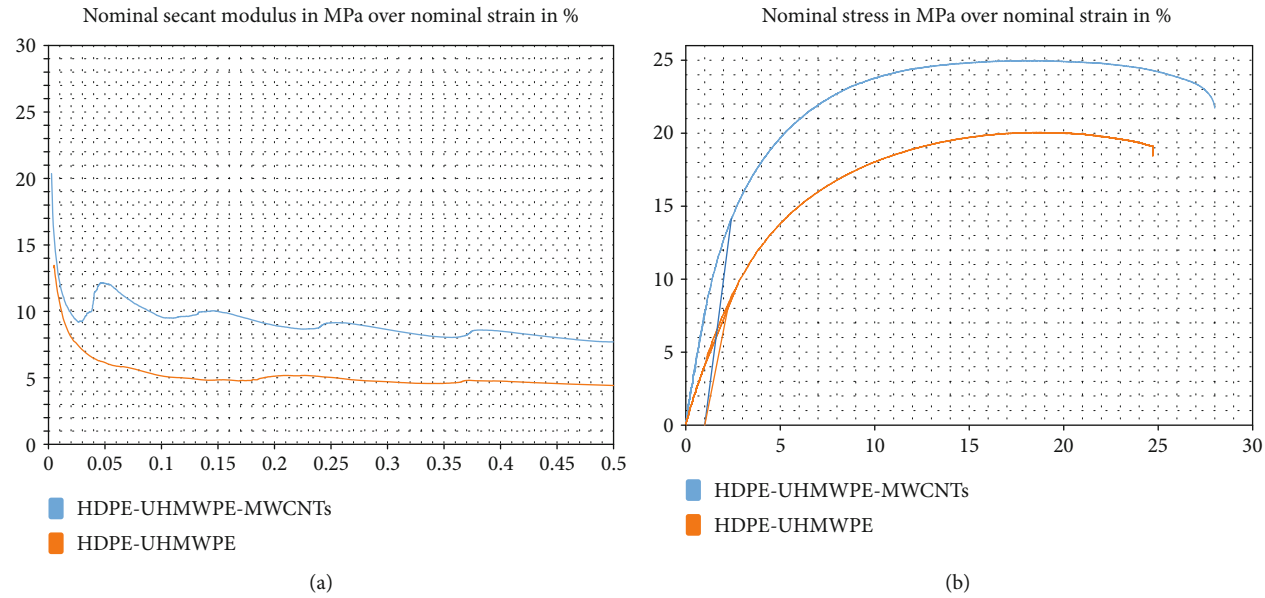

Figure 4: Tensile test presenting the stress-strain performance for HDPE-UHMWPE-MWCNTs samples and HDPE-UHMWPE, (a) Secant modulus in (MPa) over the strain in (%), while (b) present the stress in (MPa) over the strain in (%).

Table 4: Comparison results obtained from the mechanical hardness tensile test between HDPE-UHMWPE-MWCNT samples and the best sample performed HDPE-UHMWPE in Group I. Presented values correspond to the mean ± standard deviation ($\bar{X} \pm$ SD) of the data in Shore D.

HDPE-UHMWPE-MWCNTs	$\bar{X} \pm$ SD
50-50-0.0	63.00 ± 0.97
49.5-50-0.5	67.02 ± 1.10
49.0-50-1.0	65.64 ± 0.95
48.5-50-1.5	64.72 ± 0.93
48.0-50-2.0	55.92 ± 0.78
47.5-50-2.5	65.28 ± 0.74
47.0-50-3.0	64.10 ± 0.90
46.5-50-3.5	61.82 ± 1.95
46.0-50-4.0	62.78 ± 0.64
45.5-50-4.5	62.50 ± 0.53
45.0-50-5.0	54.50 ± 1.04

performed in two stages, whose results are presented in Table 5. In the first stage, when the sliding surface of inclined plane setup was from the same sample type as shown in Table 5, the inclination angle (θ) was measured from mean value of ten repetitive measurements. Then, the friction coefficient at a static position (μ^o) was measured according to the value of angle (θ). While, the second stage measurements for θ and μ^o performed when the sliding surface of the inclined plane setup was from biological surface (poultry tissue). The results showed that in both stages, the friction coefficient (μ^o) is lower for the samples including MWCNTs compared to the sample without MWCNTs. This indicates that adding MWCNTs to the polymeric sample reduces the friction properties between the surfaces. The composites combining MWCNTs to the studied polymers are highly suitable for medical applications that required low friction, such as orthopedic implants and interventional biopsy needles.

To analyze the significance of our results, we compared them with already published literature for related studies that involved a similar approach and used the concept of mixing HDPE-UHMWPE-MWCNTs. It is important to note that our work used various mixing ratios from the proposed materials to enable an extensive characterization with respect to a variety of features tested in several evaluation methods. Based on the environmental conditions and the type of devices used, they are not all available in the literature to this extent.

Our approach showed a high yield point value of 104 ± 28.70 MPa in sample 15 (48% HDPE-50% UHMWPE-2% MWCNTs) compared with the literature. Moreover, we measured a yield point of 84.2 ± 18.4 MPa in sample 13 (49% HDPE-50% UHMWPE-1% MWCVNTs) and 70 ± 21.60 MPa in sample 16 (47.5% HDPE-50% UHMWPE-2.5% UHMWPE), while a similar value for the yield point value of 78 MPa was observed for a sample composition of 98.5% UHMWPE-1.5% MWCNTs presented in [63].

The hardness test in the present study has provided relatively similar values ranging from 63 ± 0.97 to 67.02 ± 1.10 Shore D. The sample with a concentration 48.5% HDPE-50% UHMWPE-1.5% MWCNTs achieved 67.02 ± 1.10 Shore D, consistent with 67 Shore D results by using a concentration of 50% UHMWPE-48% HDPE-2% MWCNTs as presented in [32]. Furthermore, the hardness value in this work achieved 64.72 Shore D for the sample 48.5% HDPE-50% UHMWPE-1.5% MWCNTs, comparable to the

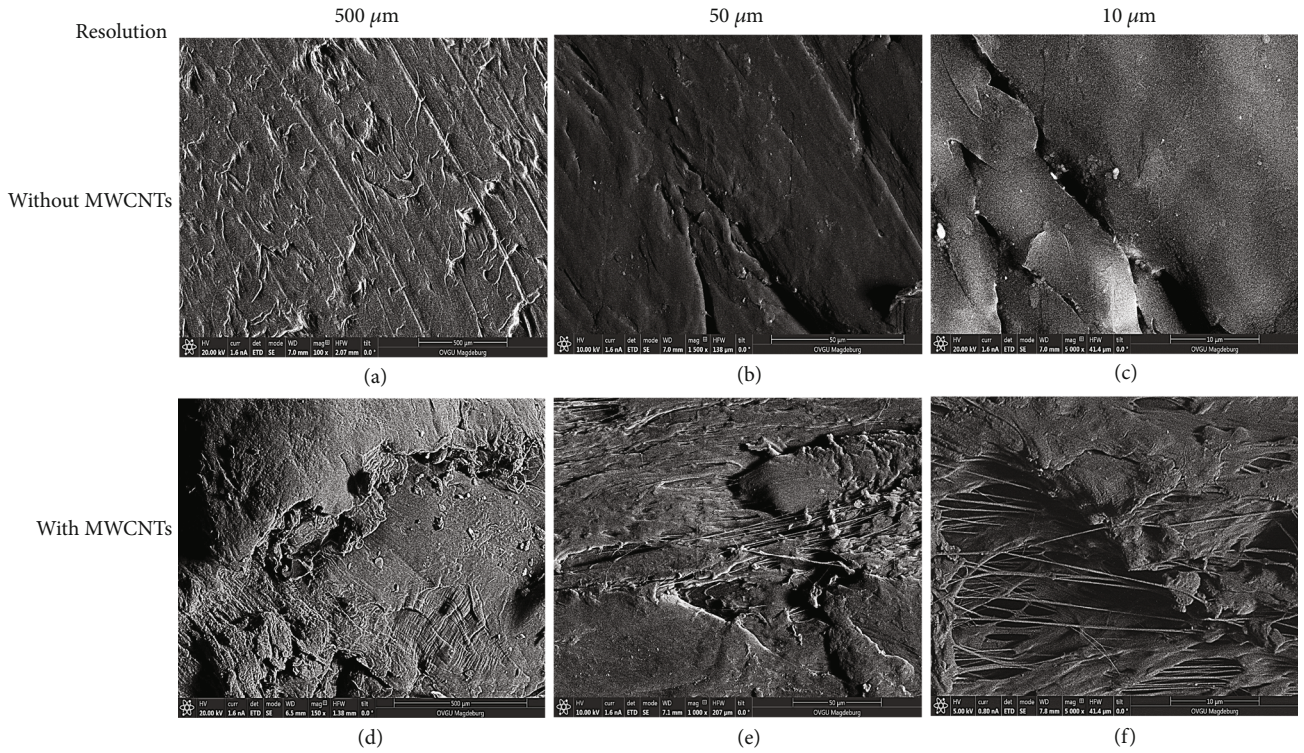

Figure 5: An overview of SEM analysis for the proposed samples with different magnification scales. The SEM images (a), (b) and (c) represent the surface characteristics for the pure polymer-polymer composites (HDPE-UHMWPE, while (d), (e), and (f) represent the microstructures of MWCNTs being added to the HDPE-UHMWPE mixture.

Table 5: Results obtained from the friction coefficient test applied to the sample from the HDPE-UHMWPE group and sample from the HDPE-UHMWPE-MWCNT group using different types of surfaces. Presented values correspond to the mean ± standard deviation ($\bar{X} \pm \mathrm{SD}$) of the data.

No.	Sample	Sliding surface	$\theta = \bar{X} \pm \mathrm{SD}$	$\mu^{o} = \tan\theta$
1	40% HDPE-60% UHMWPE	HDPE-UHMWPE	20.6 ± 3.90	0.37
		Biological surface	29.9 ± 1.90	0.57
2	46% HDPE-50% UHMWPE-4% MWCNTs	HDPE-UHMWPE-MWCNTs	14.8 ± 0.874	0.26
		Biological surface	18.9 ± 2.48	0.34

literature in sample 0.5MWCNTs-99.5% HDP, 98.75% UHMWPE-1.25% MWCNTs, 97% UHMWPE-3% MWCNTs, and 97.5% UHMWPE-2.5% MWCNTs, with 63, 64.60, 63.44, and 64.90 Shore D, respectively [14, 48, 64].

4. Conclusions

In this study, samples from HDPE-UHMWPE and HDPE-UHMWPE-MWCNTs were fabricated and evaluated based on their mechanical and tribological performance. The mass ratio for both of polyethylene used was from 100% to 95%, while for MWCNT is 0 to 5%.

The mechanical tensile and hardness measurements indicated that adding MWCNTs as reinforced material to the polymeric composite improved mechanical performance. Because it achieved promising performance in yield point, where the samples improved their ability to deform elastically and return to the original shape even under higher stress. At the same time, Young's modulus of the samples showed an increase in the stiffness property of the composites. Moreover, the ultimate tensile stress showed a remarkable increase in performance. The hardness results showed higher value leading to a better ability of samples to resist scratching and cutting. Also, the addition of MWCNTs to the studied polymeric composite led to a lower friction coefficient between surfaces. As conclusion, this work showed the synergetic effect on the polymer-polymer composites due to adding MWCNT improvement in the mechanical tensile and hardness measurements. When we vary the amount of MWCNTs and significantly increase the ratio of MWCNTs, we get more stiffness and hardness in the sample performance, due to the MWCNT that works like a bridge

for the cracks and prevents a complete separation of the two sides of the crack by forming a filament-like connection between the crack surfaces. Although we did not quantify the resulting stress redistribution along the fibers compared to a material without nanofibers, it is to expect that the fibers produce a considerable reduction of the stresses at the crack tip, which explains the larger ductility and strength of UHMWPE with nanofibers.

This phenomenon opens perspectives for the use of reinforced materials in different medical applications that require high strength, stiffness, or must be resistant to scratching with less friction coefficient, such as orthopedic implants and biopsy needles. The results of the SEM imaging revealed successful incorporation of MWCNTs in the polymeric composite matrix with homogeneous dispersion.

As future work, we propose an additional mechanical comparison combined with tribological friction tests and wear tests, especially with human tissue. Moreover, we propose to examine the designed samples in biological phantoms under image-guided therapies, such as magnetic resonance imaging, to verify the stability and the appearance of the artefact to demonstrate their suitability in interventional medical applications.

Data Availability

The data used to support the findings of this study are included within the article.

Conflicts of Interest

The authors declare that they have no conflicts of interest.

Acknowledgments

The authors would like to thank Dr. Christian Daniel, Institute of Mechanics, Chair of Technical Dynamics, Faculty of Mechanical Engineering at Otto von Guericke University Magdeburg for providing the technical support we needed to perform tensile test. Furthermore, the authors would like to thank Karsten Harnisch (MSc), Institute of Materials and Joining Technology IWF, at Otto von Guericke University Magdeburg for offering technical support to do scanning electron microscopy (SEM). This research work was coordinated between OVGU, UACh, NIS, and MTI and within their research plans 2019-2021. This work was partly funded by the research grant "Biokinetic and Physical Simulation Studies for the Design of In Vivo Imaging Pharmacokinetics" of the Ministry of Science, Energy, Climate Protection and Environment of the Federal State of Saxony-Anhalt (Germany).

Supplementary Materials

Supplementary Table S1: results obtained from the mechanical tensile test applied to the HDPE-UHMWPE, presented values correspond to the mean ± standard deviation ($\bar{X}$±SD) of the data. Supplementary Table S2: results obtained from the mechanical tensile test applied to the HDPE-UHMWPE-MWCNT samples, presented values correspond to the mean ± standard deviation ($\bar{X}$±SD) of the data. Supplementary Figure S3: SEM analysis for samples with and without addition of MWCNTs. *(Supplementary Materials)*

References

[1] G. M. Raghavendra, K. Varaprasad, and T. Jayaramudu, "Biomaterials: design, development and biomedical applications," in *Nanotechnology Applications for Tissue Engineering*, pp. 21–44, William Andrew Publishing, 2015.

[2] S. A. Shabalovskaya, "On the nature of the biocompatibility and on medical applications of NiTi shape memory and superelastic alloys," *Bio-medical Materials and Engineering*, vol. 6, no. 4, pp. 267–289, 1996.

[3] S. Petronis, *Topographic micro patterning of biomaterials using silicon templates Technical Report no. APR2000-7*, Department. of Applied Physics, Chalmers University of Technology and Göteborg University, 2000.

[4] A. Tathe, M. Ghodke, and A. P. Nikalje, "A brief review: biomaterials and their application," *International Journal of Pharmacy and Pharmaceutical Sciences*, vol. 2, no. 4, pp. 19–23, 2010.

[5] S. H. R. Ali, M. M. A. Almaatoq, and A. S. A. Mohamed, "Classifications, surface characterization and standardization of nanobiomaterials," *International Journal of Engineering & Technology*, vol. 2, no. 3, p. 187, 2013.

[6] P. Parida, A. Behera, and S. C. Mishra, "Classification of biomaterials used in medicine," *International Journal of Advances in Applied Sciences*, vol. 1, no. 3, 2012.

[7] L. G. Griffith, "Polymeric biomaterials," *Acta Materialia*, vol. 48, no. 1, pp. 263–277, 2000.

[8] C. Deepa and M. Ramesh, "Biocomposites for prosthesis," in *Green Biocomposites for Biomedical Engineering*, pp. 339–351, Woodhead Publishing, 2021.

[9] M. F. Ashby and D. R. H. Jones, *Engineering Materials 1: An Introduction To Properties, Applications And Design*, Elsevier, USA, 2012.

[10] M. Ramesh and C. Deepa, "Biocomposites for biomedical devices," in *Green Biocomposites for Biomedical Engineering*, pp. 287–300, Woodhead Publishing, 2021.

[11] M. C. Hacker, J. Krieghoff, and A. G. Mikos, "Synthetic polymers," in *Principles of regenerative medicine*, pp. 559–590, Elsevier, 2019.

[12] B. Sikora, M. Rafat, and M. J. Łos, "Examples of successful biomaterial-based artificial tissues–artificial corneas," in *Stem Cells and Biomaterials for Regenerative Medicine*, pp. 191–202, Elsevier, 2019.

[13] G. M. Swallowe, *Mechanical properties and testing of polymers: an A–Z reference*, Springer Science & Business Media, 1999.

[14] N. Camacho, S. W. Stafford, K. M. Garza, R. Suro, and K. I. Barron, "Ultra-High molecular weight polyethylene reinforced with multiwall carbon nanotubes: in vitro biocompatibility study using macrophage-like cells," *Lubricants*, vol. 3, no. 3, pp. 597–610, 2015.

[15] K. K. Ahmed, M. A. Tamer, M. M. Ghareeb, and A. K. Salem, "Recent advances in polymeric implants," *AAPS PharmSciTech*, vol. 20, no. 7, pp. 1–10, 2019.

[16] H. R. Salah, "Developed design for humeral head replacement using 3D surface mapping," *Latvian Journal of Physics and Technical Sciences*, vol. 51, no. 6, pp. 41–55, 2014.

[17] M. Borowska, A. Kot-Wasik, and J. Kucińska-Lipka, *Biopsy needles coated with the antimicrobial coatings*, Proceedings of the 15th International Students Conference "Modern Analytical Chemistry", 2019.

[18] J. A. Hibner, "Biopsy needle and method," *Google Patents*, 2009, US Patent 7,491,17.

[19] K. Modjarrad and S. Ebnesajjad, *Handbook of polymer applications in medicine and medical devices*, Elsevier, 2013.

[20] M. Hussain, R. A. Naqvi, N. Abbas et al., "Ultra-high-molecular-weight-polyethylene (UHMWPE) as a promising polymer material for biomedical applications: a concise review," *Polymers (Basel)*, vol. 12, no. 2, p. 323, 2020.

[21] Y. Xue, W. Wu, O. Jacobs, and B. Schädel, "Tribological behaviour of UHMWPE/HDPE blends reinforced with multi-wall carbon nanotubes," *Polymer Testing*, vol. 25, no. 2, pp. 221–229, 2006.

[22] J. Milisavljević, E. Petrović, I. Ćirić, M. Mančić, D. Marković, and M. Đorđević, "Tensile testing for different types of polymers," in *29th DANUBlA-ADRIA Symposium on Advances in Experimental Mechanics*, University of Belgrade, Serbia, 2012.

[23] M. A. Semeliss, R. Wong, and M. E. Tuttle, *The yield and post-yield behavior of high-density polyethylene*, Department of Mechanical Engineering, University of Washington, 1990.

[24] A. D. A. Lucas, J. D. Ambrósio, H. Otaguro, L. C. Costa, and J. A. Agnelli, "Abrasive wear of HDPE/UHMWPE blends," *Wear*, vol. 270, no. 9–10, pp. 576–583, 2011.

[25] J. Pravin, A. A. Khan, R. Massimo, R. Carlo, and T. Alberto, "Multiwalled carbon nanotube–strength to polymer composite," *Physical Sciences Reviews*, vol. 1, no. 2, 2016.

[26] S. Rehmani, M. Ahmad, M. U. Minhas, H. Anwar, and M. Sohail, "Development of natural and synthetic polymer-based semi-interpenetrating polymer network for controlled drug delivery: optimization and in vitro evaluation studies," *Polymer Bulletin*, vol. 74, no. 3, pp. 737–761, 2017.

[27] E. Enqvist, "Carbon nanofiller reinforced UHMWPE for orthopaedic applications: optimization of manufacturing parameters," *Luleå Tekniska Universitet*, 2013, US Patent 7,491,17.

[28] B. McKelvogue, "Improvements to UHMWPE," *Journal of Undergraduate Research (JUR) at Minnesota State University, Mankato*, vol. 10, no. 1, p. 5, 2010.

[29] M. Ziąbka, A. Mertas, W. Król, A. Bobrowski, and J. Chłopek, "High density polyethylene containing antibacterial silver nanoparticles for medical applications," *Macromolecular Symposia*, vol. 315, no. 1, pp. 218–225, 2012.

[30] A. S. Mohammed, "UHMWPE nanocomposite coatings reinforced with alumina (Al2O3) nanoparticles for tribological applications," *Coatings*, vol. 8, no. 8, p. 280, 2018.

[31] E. Enqvist, D. Ramanenka, P. A. A. P. Marques, J. Gracio, and N. Emami, "The effect of ball milling time and rotational speed on ultra high molecular weight polyethylene reinforced with multiwalled carbon nanotubes," *Polymer Composites*, vol. 37, no. 4, pp. 1128–1136, 2016.

[32] A. Ma, Y. Wu, W. Chen, and X. Wu, "Preparation and properties of multi-walled carbon nanotubes/carbon fiber/epoxy composites," *Polymer Composites*, vol. 35, no. 11, pp. 2150–2153, 2014.

[33] M. A. Samad and S. K. Sinha, "Nanocomposite UHMWPE–CNT polymer coatings for boundary lubrication on aluminium substrates," *Tribology Letters*, vol. 38, no. 3, pp. 301–311, 2010.

[34] S. R. Bakshi, J. E. Tercero, and A. Agarwal, "Synthesis and characterization of multiwalled carbon nanotube reinforced ultra high molecular weight polyethylene composite by electrostatic spraying technique," *Composites. Part A, Applied Science and Manufacturing*, vol. 38, no. 12, pp. 2493–2499, 2007.

[35] M. U. Azam and M. A. Samad, "A novel organoclay reinforced UHMWPE nanocomposite coating for tribological applications," *Progress in Organic Coatings*, vol. 118, pp. 97–107, 2018.

[36] M. Rouway, M. Nachtane, M. Tarfaoui et al., "Mechanical properties of a biocomposite based on carbon nanotube and graphene nanoplatelet reinforced polymers: analytical and numerical study," *Journal of Composites Science*, vol. 5, no. 9, p. 234, 2021.

[37] F. Azimpour-Shishevan, H. Akbulut, and M. A. Mohtadi-Bonab, "Synergetic effects of carbon nanotube and graphene addition on thermo- mechanical properties and vibrational behavior of twill carbon fiber reinforced polymer composites," *Polymer Testing*, vol. 90, article 106745, 2020.

[38] S. H. R. Ali and B. S. N. Azzam, "Mechanical, tribological properties and surface characteristics of developed polymeric materials reinforced by CNTs," *SAE International Journal of Fuels and Lubricants*, vol. 8, no. 1, pp. 35–40, 2015.

[39] S. Dabees, V. Tirth, A. Mohamed, and B. M. Kamel, "Wear performance and mechanical properties of MWCNT/HDPE nanocomposites for gearing applications," *Journal of Materials Research and Technology*, vol. 12, pp. 2476–2488, 2021.

[40] M. Z. Hussain, S. Khan, R. Nagarajan, U. Khan, and V. Vats, "Fabrication and microhardness analysis of MWCNT/MnO2 nanocomposite," *Journal of Materials*, vol. 2016, Article ID 6070468, 2016.

[41] S. S. Khasraghi and M. Rezaei, "Preparation and characterization of UHMWPE/HDPE/MWCNT melt-blended nanocomposites," *Journal of Thermoplastic Composite Materials*, vol. 28, no. 3, pp. 305–326, 2015.

[42] J. V. Veetil and K. Ye, "Tailored carbon nanotubes for tissue engineering applications," *Biotechnology Progress*, vol. 25, no. 3, pp. 709–721, 2009.

[43] J. Simon, E. Flahaut, and M. Golzio, "Overview of carbon nanotubes for biomedical applications," *Materials (Basel)*, vol. 12, no. 4, p. 624, 2019.

[44] A. B. Tekinay, "Nanomaterials for Regenerative Medicine," in *Stem Cell Biology and Regenerative Medicine*, pp. 1–45, Springer, Switzerland, 2019.

[45] S. H. R. Ali, M. K. Bedewy, M. A. Etman, H. A. Khalil, and B. S. Azzam, "Morphology and properties of polymer matrix nanocomposites," *International Journal of Metrology and Quality Engineering*, vol. 1, no. 1, pp. 33–39, 2010.

[46] A. Eatemadi, H. Daraee, H. Karimkhanloo et al., "Carbon nanotubes: properties, synthesis, purification, and medical applications," *Nanoscale Research Letters*, vol. 9, no. 1, pp. 1–13, 2014.

[47] N. Camacho, E. A. Franco-Urquiza, and S. W. Stafford, "Wear performance of multiwalled carbon nanotube-reinforced ultra-high molecular weight polyethylene composite," *Advances in Polymer Technology*, vol. 37, no. 6, 2269 pages, 2018.

[48] D. Lawal, A. Bin Ali, and A. S. Mohammed, "Tribological investigations of carbon nanotube-reinforced polymer (UHMWPE) nanocomposites using Taguchi methodology," *Journal of Applied Polymer Science*, vol. 133, no. 40, 2016.

[49] M. Hosseini, M. Ghalenovi, M. Pourafshari Chenar, S. A. Mousavi, H. R. Afshoon, and S. R. Ghafarian, "The effect of MWCNT on the mechanical and electrical properties of HDPE/MWCNT nanocomposite," *The 7th International Chemical Engineering Congress & Exhibition*, 2011, US Patent 7,491,17.

[50] T. Yu and G. L. Wilkes, "Influence of molecular weight distribution on the melt extrusion of high density polyethylene (HDPE): effects of melt relaxation behavior on morphology and orientation in HDPE extruded tubular films," *Journal of Rheology*, vol. 40, no. 6, pp. 1079–1093, 1996.

[51] J. I. Yoon, J. G. Kim, J. M. Jung et al., "Obtaining reliable true plastic stress-strain curves in a wide range of strains using digital image correlation in tensile testing," *Korean Journal of Metals and Materials*, vol. 54, no. 4, pp. 231–236, 2016.

[52] T. S. Chow, "Stress–strain behavior of polymers in tension, compression, and shear," *Journal of Rheology*, vol. 36, no. 8, pp. 1707–1717, 1992.

[53] J. Pelleg, *Mechanical properties of materials*, Springer Science & Business Media, 2013.

[54] S. Zherebtsov, I. P. Semenova, H. Garbacz, and M. Motyka, "Advanced mechanical properties," in *Nanocrystalline Titanium*, pp. 103–121, Elsevier, 2019.

[55] B. B. Muvdi and J. W. McNabb, *Engineering Mechanics Of Materials*, Springer Science & Business, 2012.

[56] D. Roylance, "Mechanical properties of materials," *Massachusetts Institute of Technology*, pp. 51–78, 2008, US Patent 7,491,17.

[57] M. Andó, G. Kalácska, and T. Czigány, "Shore d hardness of cast pa 6 based composites," *Scientific Bulletin Series C: Fascicle Mechanics, Tribology, Machine Manufacturing Technology*, vol. 23, no. 15, p. 2009, 2009.

[58] S. H. R. Ali, "Advanced nanomeasuring techniques for surface characterization," *International Scholarly Research Notices*, vol. 2012, Article ID 859353, 23 pages, 2012.

[59] S. H. R. Ali, M. M. A. Almaatoq, and A. S. A. Mohamed, "Recent progress in nanometrology techniques for object characterization," *International Journal of Engineering Research and Applications (IJERA)*, vol. 3, no. 4, pp. 1343–1366, 2013.

[60] M. Ahmad, M. U. Wahit, M. R. A. Kadir, K. Z. M. Dahlan, and M. Jawaid, "Thermal and mechanical properties of ultrahigh molecular weight polyethylene/high-density polyethylene/polyethylene glycol blends," *Journal of Polymer Engineering*, vol. 33, no. 7, pp. 599–614, 2013.

[61] A. Peacock, *Handbook Of Polyethylene: Structures: Properties, And Applications*, CRC press, 2000.

[62] R. D. Ibrahim Dickey, R. L. Jackson, and G. T. Flowers, "Measurements of the static friction coefficient between tin surfaces and comparison to a theoretical model," *Journal of Tribology*, vol. 133, no. 3, article 031408, 2011.

[63] B. M. Amoli, S. A. A. Ramazani, and H. Izadi, "Preparation of ultrahigh-molecular-weight polyethylene/carbon nanotube nanocomposites with a Ziegler–Natta catalytic system and investigation of their thermal and mechanical properties," *Journal of Applied Polymer Science*, vol. 125, no. S1, pp. E453–E461, 2012.

[64] J. Wang, C. Cao, X. Chen et al., "Orientation and dispersion evolution of carbon nanotubes in ultra high molecular weight polyethylene composites under extensional-shear coupled flow: a dissipative particle dynamics study," *Polymers (Basel)*, vol. 11, no. 1, p. 154, 2019.